This paper can be cited as: Tseng, I. M., Liu, T. Y., Pan, Y. H., Hsu, P. E., Ou, W. E., Jiang, P. Y. & Yang, W. L. (2024). Simulating Molecular Optical Properties of Polyimide for Non-volatile Resistive Photomemory Devices. MATTER: International Journal of Science and Technology, 10, 13-26.

SIMULATING MOLECULAR OPTICAL PROPERTIES OF POLYIMIDE FORNONVOLATILE RESISTIVE PHOTOMEMORY DEVICES

I-Ming Tseng

Department of Electronic Engineering Feng Chia UniversityTaichung, 40724, Taiwan
aa324243@gmail.com

Tang-Yi Liu

Department of Electronic Engineering Feng Chia UniversityTaichung, 40724, Taiwan
psbabytiger52@gmail.com

Yi-Huan Pan

Department of Electronic Engineering Feng Chia UniversityTaichung, 40724, Taiwan
a37649089@gmail.com

Pin-En Hsu

Department of Electronic Engineering Feng Chia UniversityTaichung, 40724, Taiwan
toby26294090@gmail.com

Wei-Cheng Ou

Department of Electronic Engineering Feng Chia UniversityTaichung, 40724, Taiwan
w0988801009@gmail.com

Pei-Ying Jiang

Department of Electronic Engineering Feng Chia UniversityTaichung, 40724, Taiwan
pei199812@gmail.com

Wen-Luh Yang

Department of Electronic Engineering Feng Chia UniversityTaichung, 40724, Taiwan
wlyang@fcu.edu.tw

Abstract

In this study, the focus was on utilizing the polyimide (PI) thin film as a resistive conversion layer for organic polyimide-based resistive random-access memory (ReRAM) applications. We utilized the 3D molecular editor WebMO to manipulate and analyze the structures of Aromatic-PI and Quinoid-PI molecules. The molecular chain length, molecular weight, and HOMO/LUMO molecular orbitals were investigated to gain insights into the fundamental properties of PI molecular structures. The analysis revealed that the Quinoid-PImolecule exhibited a shorter molecular chain compared to Aromatic-PI, attributed to the inability of the cyclic structure in Quinoid-PI to maintain a planar conjugated structure, resulting in an uneven overall structure and reduced molecular chain length (Norcorss, 1988). The research results demonstrate that the optical energy gap of Aromatic-PI remains constant regardless of the number of molecular bonds, with a value of approximately 3.2661 eV. In contrast, for Quinoid-PI, the optical energy gap undergoes a significant decrease as the number of molecular bonds ranges from 1 to 5. As the bond count increases to 20~23, thechange in the optical energy gap gradually diminishes, ultimately resulting in an optical energy gap of 0.6932 eV. This observation indicates that longer molecular chains composed of Aromatic-PI act as insulators, while Quinoid-PI transforms into a low-energy gap conductor.

Keywords

Nonvolatile, Photomemory, Polyimide, Simulation

1. Introduction

With the rapid development of our generation, artificial intelligence, big data, and theInternet of Things have become the prevailing technological trends (Yuan, Liu, Chen, Fan, & Liu, 2021). These advancements necessitate extensive information processing, making memory an essential component in electronic products.

Given that flash memory is approaching its size reduction limit. The development ofthe new generation of non-volatile memory is being actively pursued. The new generation of memories includes Ferroelectric Random Access Memory (FeRAM), Magnetoresistive Random Access Memory (MRAM), Phase Change Memory (PCRAM), and Resistive Random Access Memory (ReRAM) (Aswathy & Sivamangai, 2021; Meena, Sze, Chand, & Tseng,

2014). Among them, ReRAM stands out due to its strong flexibility, cost-effectiveness, using simple techniques, simple structure, fast switching speed, low operating voltage, excellent durability, reliable data retention, and low power consumption (Gao, Song, Chen, Zeng, & Pan, 2012; Ouyang, Chu, Tseng, Prakash, & Yang, 2005). To address the challenges associated with component scaling. We have implemented the structure of RRAM and incorporated a charge transfer mechanism. To ensure the preservation of excellent component characteristics during the scaling process. Both academia and the semiconductor industry have high hopes for the development of ReRAM. Because photomemory offers significantly higher read and write speeds and device densities compared to conventional memories, it shows great potential.

A wide variety of organic materials exists, with polyimides garnering recent research attention from multiple teams. Polyimide stands out among other organic polymer materials. due to its excellent physical and chemical properties, including heat resistance, insulation, chemical corrosion resistance, good tensile strength, and photosensitivity (Gouzman et al., 2019; Ling et al., 2006; Mu, Hsu, Kuo, Han, & Zhou, 2020; Zhao, Zhang, Wan, Yang, & Hwang, 2018). To address the challenges associated with device scaling. We implemented the structure of RRAM and incorporated a charge transfer mechanism to ensure the maintenance of excellent device characteristics during scaling (Gouzman et al., 2019; Yen &Liou, 2012).

Through chemical synthesis, our team formed polyimide using organic materials and applied it to memory operations. Polyimide serves as a resistance conversion layer, capable of changing its resistance value by receiving different forms of energy (Slesazeck & Mikolajick, 2019; Xiao et al., 2015; Zan & Kao, 2009). Initially, all PI films are in the high- resistance state (HRS). However, when a voltage or an ultraviolet light source is applied to the film.it undergoes a transformation from an aromatic compound with a higher energy gap to a quinoid compound with a lower energy gap, resulting in a low- configured low-resistance state (LRS) (see Figure 1).

The charge transfer mechanism relies on the molecular structure conversion between PI films, enabling changes in resistance value. As a result, the film can be switched between high resistance and low resistance states, facilitating the functions of writing, and erasing in the memory system (García, García, Serna, & de la Peña, 2010; Ren et al., 2013) .

In this study, we conducted an analysis of the molecular structures within polyimide using simulation software to investigate the changes in energy gaps between molecules. Polyimide undergoes alterations in its chemical structure during energy conversion, transitioning between high and low configurations. To gain a deeper understanding of these

variations, we utilized the simulation software to collect and analyze various data related to the molecular structures within polyimide.
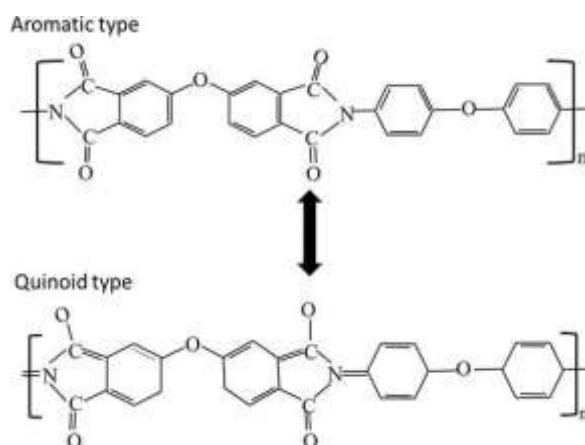

Figure 1: *Schematic Diagram of Conversion of Aromatic-PI Structure into Quinoid-PI Structure*
(Source: Self/Authors' Own Illustration)

2. Materials and Experimental Methods

2.1. Materials:

The monomer ODA (diamine) and ODPA (dianhydride) used in this study were purchased from Jingming Chemical Co., Ltd. Additionally, the solvent NMP (N-Methyl-2-pyrrolidone) was also obtained from Jingming Chemical Co., Ltd. These chemicals were selected for their suitability in the synthesis and preparation of the polyimide materials used in our experiments.

2.2. Experimental Methods:

The preparation of the solution was carried out in a nitrogen-filled glove box. Firstly, the powdered 4,4'-Oxydiphthalic anhydride (ODPA) was added to a solution of 1-methyl-2-pyrrolidone (NMP) and stirred for 30 minutes. Subsequently, the granular 4,4'-oxydianiline (ODA) was added, and the stirring continued for 12 hours. Finally, the prepared viscous polyimide acid solution (PAA) was stored at low temperature to ensure quality. In this paper, the research team prepared a 15% concentration PAA solution.

After the solution was prepared, it was coated onto TaN metal by using a spin coater to achieve a uniform coating. Initially, the first spin coating was performed at a pre-spin speed of 500 rpm for 10 seconds, followed by a spin speed of 3000 rpm for 30 seconds. After the spin coating, the samples were placed in an oven and gradually heated to 260 degrees Celsius for curing (Figure 2). During this curing process, the PAA molecules underwent dehydration

cyclization to form a PI film, which is referred to as imidization. After the sample has been cooled, it is removed from the oven and a metal mask is attached. A layer of 100 nm-thick aluminum is then evaporated onto the sample surface to serve as the upper electrode, forming a sandwich structure of TaN/PI/Al and completing the element fabrication process.
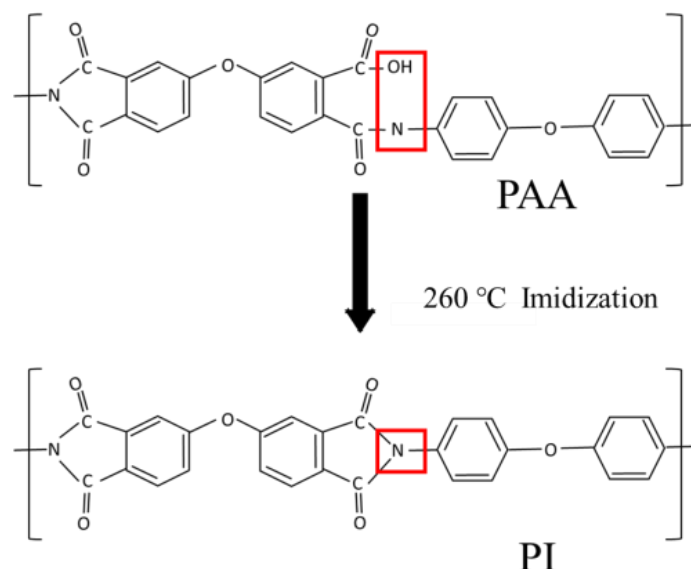

Figure 2: *Schematic 260°C Imidization to Form PI Films*
(*Source: Self/Authors' Own Illustration*)

2.3. Simulation Software:

WebMO is a versatile and user-friendly 3D molecular editor that offers a range of features through a web-based interface. It is compatible with popular web browsers like Edge, Chrome, Safari, and Firefox, as well as mobile devices running iOS or Android. With WebMO, users can edit and manipulate 3D molecular structures, visualize chemical calculation results, and perform molecular structure geometry optimization.

One of the notable advantages of WebMO is its integration with various professional chemical calculation software, including Gaussian, Gamess, NWChem, Orca, and Q-Chem. This allows users to seamlessly utilize different calculation engines for their research needs. WebMO's visual interface presents molecular structures, calculation results, and animations in a user-friendly manner. This makes it particularly suitable for researchers who may be new to computational chemistry or require a simplified workflow. The software's support for multiple chemical calculation software also enables efficient execution of concurrent chemistry calculation projects ("WebMO,").

In this study, the 3D molecular editor WebMO was used to edit the molecular structure of polyimide (PI) and set up the desired calculation types. The edited molecules,

along with the chosen calculation types, were then used in conjunction with quantumchemical calculation software such as Gaussian, Orca, and NWChem, to perform a series of simulations to predict chemical reactions and structural changes of the molecules. The software was also utilized to simulate the HOMO/LUMO positions and energy levels of the materials.

Prior to conducting various chemical simulations, the edited molecules underwent twoprocesses: molecular structure geometry optimization and idealization. Molecular structure idealization involves assigning reasonable bonds to each atom and adjusting bond lengths and angles to appropriate positions. Subsequently, the geometry optimization process, also known as energy minimization in the field of chemical calculations, was performed. This stepensured that during spectroscopic simulations, the molecules were not affected by interatomic interactions. As shown in the figure, both structures reached a local energy minimum in the molecular interactions before spectroscopic simulations (Polik & Schmidt, 2022).

3. Results and Discussion

Due to PI contains aromatic ring structures, making it photosensitive. It demonstrates high absorption rates for specific light sources, and under irradiation at specific wavelengths, it undergoes electron transitions in its chemical bonds, resulting in the conversion of the molecular structure from the high-energy state of Aromatic-PI to the low-energy state of Quinoid-PI. Both structures were simulated using software to visualize their respective HOMO/LUMO orbitals in Figure 3 and 4. From Figure 3, it can be found that the molecular chain of Quinoid-PI is shorter than that of Aromatic-PI. Because the ring structure in the molecular structure of Quinoid-PI cannot maintain a planar conjugated structure, which causes the molecular orbitals to interact and make the overall structure relatively weak.

Figure 4 observations showing that when PI absorbs a light source of a specific frequency and transitions from HOMO to LUMO, the ring structure in the molecular changes.

To identify the differences in the IR and UV-VIS spectra between the two molecular structures, Gaussian was employed to simulate the IR spectra of Aromatic-PI and Quinoid-PI. The simulation of molecular IR spectra enables the observation of specific peaks, which indicate the presence of functional groups in the molecular structure. By combining WebMO, the vibration modes of each functional group can be visualized, providing a clearer understanding of the molecular vibrations resulting from infrared absorption (Figure 5). By comparing the simulated IR spectra with the functional group assignments in Table 1, noticeable differences can be observed. Aromatic-PI exhibits higher peaks in the range of 1820-

1720 cm-1 (C=O) and 1400-1266 cm-1 (C-N), while Quinoid-PI shows higher peaks in the range of 1700-1610 cm-1 (C=N) and 1250-1085 cm-1 (C-O). These results align with the characteristic functional group vibration modes of Aromatic-PI and Quinoid-PI, allowing the simulated IR spectra to serve as a reference for future FTIR spectroscopy. This facilitates the
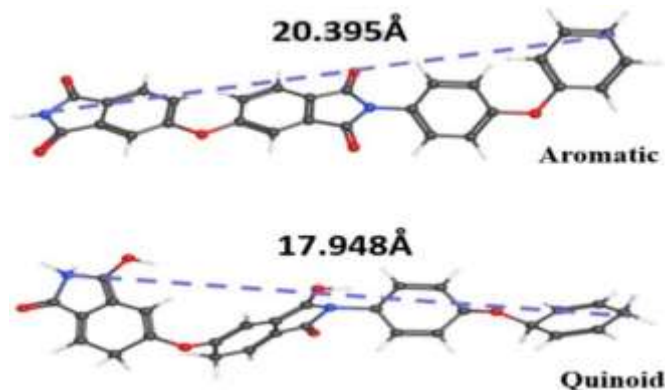
identification of molecular structural peak differences in PI films before and after light exposure.

Figure 3: *Molecular Structure Simulations of Aromatic-PI and Quinoid-PI*
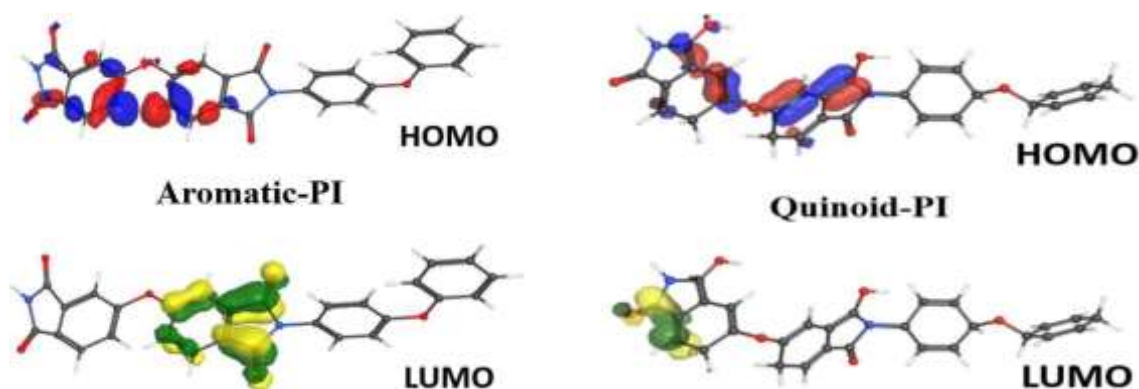*(Source: Self/Authors' Own Illustration)*

Figure 4. *Schematic diagrams of the Highest Occupied Molecular Orbital (HOMO) and Lowest Unoccupied Molecular Orbital (LUMO) of Aromatic-PI and Quinoid-PI*
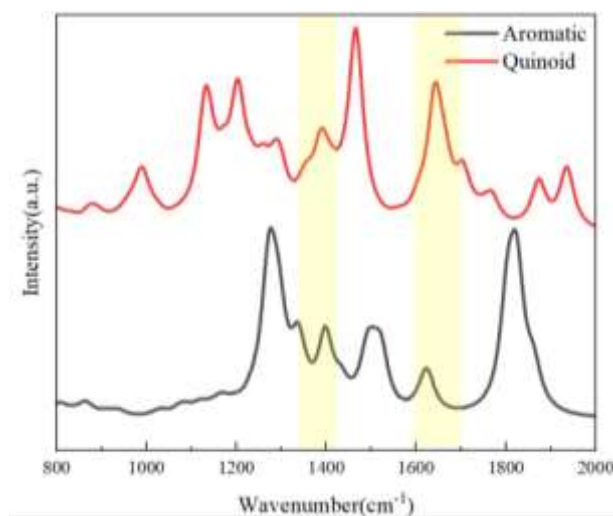*(Source: Self/Authors' Own Illustration)*

Figure 5: *IR Spectrum Simulation of Polyimide (a) Aromatic (Aromatic-PI) (b) Quinoid*
(Quinoid-PI)
(Source: Self/Authors' Own Illustration)

Table 1: Polyimide IR Simulation Spectrum and Functional Group Comparison Table

	Absorption (cm⁻¹)	*Functional Group*
(1)	1820~1720	C=O stretching
(2)	1700~1610	C=N stretching
(3)	1400~1266	C-N stretching
(4)	1250~1085	C-O、C-O-C stretching

(Source: Authors' Own Illustration)

Based on previous studies on infrared spectroscopy, it has been observed that polyimide(PI) films consist of both Aromatic-PI and Quinoid-PI molecular structures, and these structures mutually influence the film's light absorption. To investigate the photoexcitation of PI with different molecular structures, Gaussian software was employed to calculate the UV-Vis spectra of Aromatic-PI and Quinoid-PI separately, utilizing Time-dependent Density Functional Theory(TD-DFT) (Assadi & Hanaor, 2013; Sham & Kohn, 1966).

In the UV-Vis simulation of Aromatic-PI, the number of molecular bonds was found to be a crucial factor affecting the simulated results. Figure 5 demonstrates that as the number of molecular bonds increases, the absorption peak remains within the same range (~290 nm). This indicates that the aromatic ring structure of Aromatic-PI exhibits significant absorption in the UVB range (280-320 nm). The stable conjugated structure formed by the aromatic rings allows the electrons to stay in the same plane, minimizing the impact of the increased Pauli

Exclusion Principle due to additional molecular bonds.

Contrarily, the UV-Vis simulation of Quinoid-PI reveals a redshift in the absorption peak as the number of molecular bonds increases, as depicted in Figure 6(a). This suggests the presenceof an unstable non-planar conjugated structure in Quinoid-PI. The increased Pauli Exclusion Principle resulting from the additional molecular bonds affects the positions of the Highest Occupied Molecular Orbital (HOMO) and Lowest Unoccupied Molecular Orbital (LUMO) of Quinoid-PI, as shown in Figure 6(b), leading to the observed redshift in the UV-Vis spectrum. This shift influences the bandgap and other physical properties of the material. The graph illustrates that the HOMO-LUMO gap continuously decreases with an increasing number of molecular bonds until it reaches a saturation point at approximately 23 bonds.

Subsequently, the UV-Vis spectra of the two PI molecular structures were compared at different bond counts, and the optical bandgap of each structure was calculated by determining theintersection of the tangent line at the maximum absorption wavelength and the wavelength itself, using the following formula:

$$\boldsymbol{Eg(eV) = 1240\,\lambda\,(\mathbf{nm})} \quad (1)$$

The results from Figure 7 show that the optical bandgap of Aromatic-PI remains constant at approximately 3.2661 eV as the number of bonds increases. In contrast, the optical bandgap of Quinoid-PI decreases significantly from 1 to 5 bond counts. However, as the bond count reaches 20 to 23, the change in the optical bandgap becomes less pronounced, resulting in an optical bandgap of 0.6932 eV. This graph clearly illustrates that Aromatic-PI behaves as an insulator at high bond counts, while Quinoid-PI transitions to a low-bandgap conductor after exposure to UVB light.
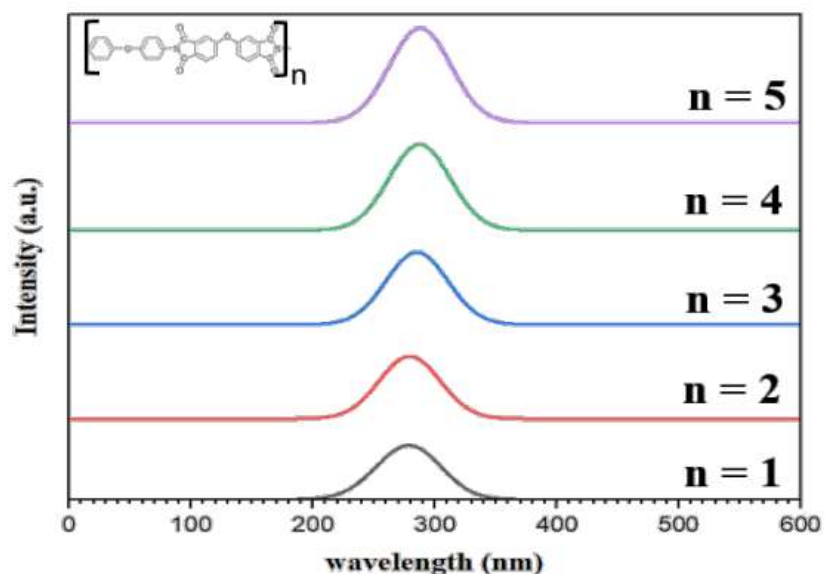
Figure 6: *UV-Vis Simulation Diagram Illustrating the Variation in Molecular Bond Numbers of Aromatic Polyimide (Aromatic-PI)*
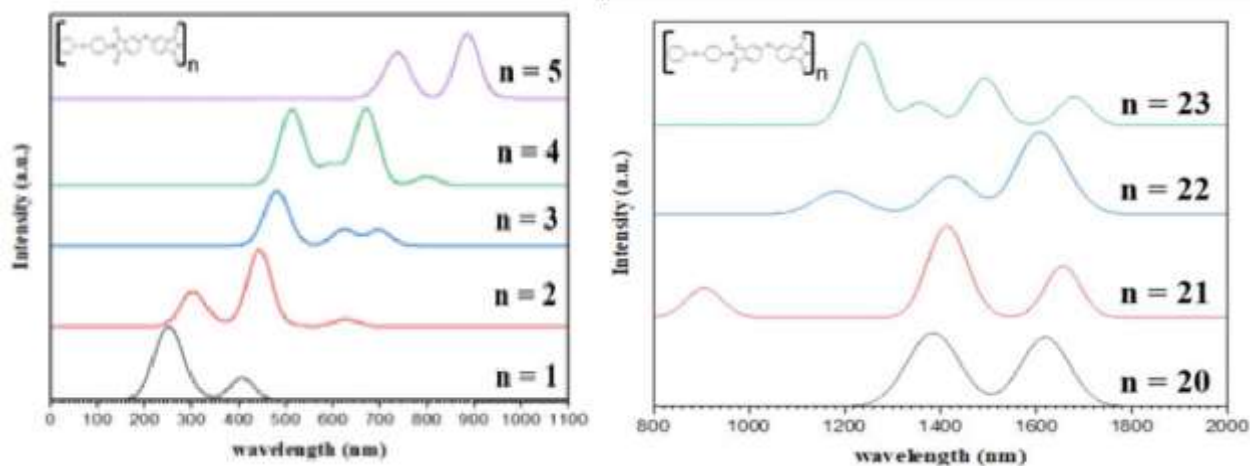*(Source: Self/Authors' Own Illustration)*

Figure 7: *UV-Vis Simulation Diagram Illustrating the Variation in Molecular Bond Numbers of Quinoid Polyimide (Quinoid-PI)*
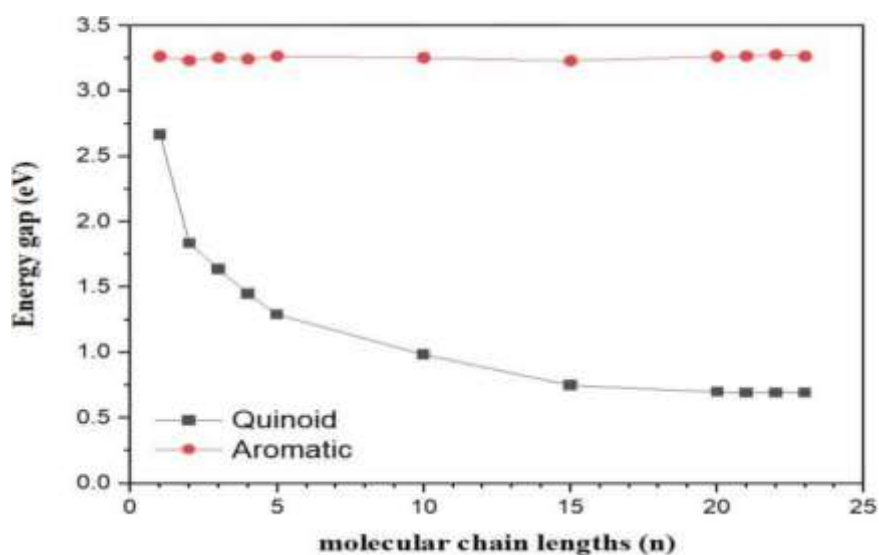*(Source: Self/Authors' Own Illustration)*

Figure 8: *The Relationship between the Number of Molecular Bonds and the Optical Energy Gap*
(Source: Self/Authors' Own Illustration)

4. Conclusion

In this study, our focus was on investigating the molecular structural variations of polyimide (PI) and simulating the infrared (IR) and UV-Vis spectra of two specific molecular structures within PI: Aromatic-PI and Quinoid-PI. To carry out these simulations, we employed the quantum chemistry software Gaussian. Through the IR spectrum simulation,we were able to identify the vibrational modes associated with specific peaks and establish the characteristic peaks of Aromatic-PI in the range of 1820-1720 cm-1 (C=O), while Quinoid-PI exhibited characteristic peaks in the range of 1700-1610 cm-1 (C=N).

Moving on to the UV-Vis simulation, we observed distinct effects of the bond count on Aromatic-PI and Quinoid-PI. We explained the redshift in the UV-Vis spectrum and the decrease in the optical band gap of Quinoid-PI with an increasing bond count by considering the influence of the Pauli Exclusion Principle. Based on the insights gained from these simulations, our future research aims to further enhance the performance of this thin film. Our objective is to enhance the optical operating capabilities, ultimately contributing to advancements in various applications.

The design of an appropriate HOMO/LUMO energy gap can be accomplished in this manner. The objective for the future is to produce low-resistance PI films with an energy gap ranging between 0.62 eV to 1.2 eV. This will be achieved by regulating the PI film processing and developing hybrid polymer materials.

ACKNOWLEDGMENTS

AUTHOR DECLARATIONS

The authors declare that there is no conflict of interest regarding the publication of this paper.

REFERENCES

Assadi, M. H., & Hanaor, D. A. (2013). Theoretical study on copper's energetics and magnetism in TiO2polymorphs. *Journal of Applied Physics, 113*(23). https://doi.org/10.1063/1.4811539

Aswathy, N., & Sivamangai, N. (2021). *Future nonvolatile memory technologies: challenges and applications.* Paper presented at the 2021 2nd International Conference on Advances in Computing,Communication, Embedded and Secure Systems (ACCESS). https://doi.org/10.1109/ACCESS51619.2021.9563288

Gao, S., Song, C., Chen, C., Zeng, F., & Pan, F. (2012). Dynamic processes of resistive switching in metallic filament-based organic memory devices. *The Journal of Physical Chemistry C, 116*(33),17955-17959. https://doi.org/10.1021/jp305482c

García, J. M., García, F. C., Serna, F., & de la Peña, J. L. (2010). High -performance aromatic polyamides. *Progress in Polymer Science, 35*(5), 623-686. https://doi.org/10.1016/j.progpolymsci.2009.09.002

Gouzman, I., Grossman, E., Verker, R., Atar, N., Bolker, A., & Eliaz, N. (2019). Advances in polyimide-based materials for space applications. *Advanced Materials, 31*(18), 1807738. https://doi.org/10.1002/adma.201807738

Ling, Q.-D., Chang, F.-C., Song, Y., Zhu, C.-X., Liaw, D.-J., Chan, D. S.-H. . . . Neoh, K.-G. (2006). Synthesis and dynamic random access memory behavior of a functional polyimide. *Journal of theAmerican Chemical Society, 128*(27), 8732-8733. https://doi.org/10.1021/ja062489n

Meena, J. S., Sze, S. M., Chand, U., & Tseng, T.-Y. (2014). Overview of emerging nonvolatile memorytechnologies. *Nanoscale research letters, 9*, 1-33. https://doi.org/10.1186/1556-276X-9-526

Mu, B., Hsu, H.-H., Kuo, C.-C., Han, S.-T., & Zhou, Y. (2020). Organic small molecule-

based RRAM for data storage and neuromorphic computing. *Journal of Materials Chemistry C, 8*(37), 12714-12738. https://doi.org/10.1039/D0TC02116D

Norcorss, B. E. (1988). Advanced organic chemistry: reactions mechanisms, and structure (Mach, Jerry). *Journal of Chemical Education, 65*(5), A139. https://doi.org/10.1021/ed065pA139.2

Ouyang, J., Chu, C.-W., Tseng, R. J.-H., Prakash, A., & Yang, Y. (2005). Organic memory devicefabricated through solution processing. *Proceedings of the IEEE, 93*(7), 1287-1296. https://doi.org/10.1109/JPROC.2005.851235

Polik, W. F., & Schmidt, J. (2022). WebMO: Web-based computational chemistry calculations in educationand research. *Wiley Interdisciplinary Reviews: Computational Molecular Science, 12*(1), e1554. https://doi.org/10.1002/wcms.1554

Ren, W., Zhu, Y., Ge, J., Xu, X., Sun, R., Li, N. . . . Lu, J. (2013). Bistable memory devices with lowerthreshold voltage by extending the molecular alkyl-chain length. *Physical Chemistry Chemical Physics, 15*(23), 9212-9218. https://doi.org/10.1039/c3cp51290h

Sham, L. J., & Kohn, W. (1966). One-particle properties of an inhomogeneous interacting electron gas. *Physical Review, 145*(2), 561. https://doi.org/10.1103/PhysRev.145.561

Slesazeck, S., & Mikolajick, T. (2019). Nanoscale resistive switching memory devices: a review. *Nanotechnology, 30*(35), 352003. https://doi.org/10.1088/1361-6528/ab2084

WebMO. Retrieved from https://www.webmo.net/

Xiao, X., Kong, D., Qiu, X., Zhang, W., Liu, Y., Zhang, S., . . . Leng, J. (2015). Shape memory polymerswith high and low temperature resistant properties. *Scientific Reports, 5*(1), 14137. https://doi.org/10.1038/srep14137

Yen, H.-J., & Liou, G.-S. (2012). Solution-processable triarylamine-based electroactive high performancepolymers for anodically electrochromic applications. *Polymer Chemistry, 3*(2), 255-264. https://doi.org/10.1039/C1PY00346A

Yuan, L., Liu, S., Chen, W., Fan, F., & Liu, G. (2021). Organic memory and memristors: from mechanisms,materials to devices. *Advanced Electronic Materials, 7*(11), 2100432. https://doi.org/10.1002/aelm.202100432

Zan, H.-W., & Kao, S.-C. (2009). New organic phototransistor with bias-modulated photosensitivity andbias-enhanced memory effect. *IEEE Electron Device Letters,*

30(7), 721-723. https://doi.org/10.1109/LED.2009.2021867

Zhao, J., Zhang, M., Wan, S., Yang, Z., & Hwang, C. S. (2018). Highly flexible resistive switching memory based on the electronic switching mechanism in the Al/TiO2/Al/polyimide structure. *ACSApplied Materials & Interfaces, 10*(2), 1828-1835. https://doi.org/10.1021/acsami.7b16214